Aerodynamic study of airfoils geometric imperfections at low Reynolds number

Rodolfo Sant [a], Luis Ayuso [b], Jose Meseguer [c]

[a] *Universidad Politecnica de Madrid, Madrid, Spain, rodolfo.sant@upm.es*
[b] *Universidad Politecnica de Madrid, Madrid, Spain, luis.ayuso@upm.es*
[c] *Universidad Politecnica de Madrid, Madrid, Spain, j.meseguer@upm.es*

1 INTRODUCTION

The interest of this study is based on the observation that some manufacturing processes of various vehicles wings, such as unmanned aerial vehicle (UAV), or blades, such as wind turbine blades, or other devices that use aerodynamic profiles, produce imperfections in the leading edge or open trailing edge with bigger thickness than original airfoil, because, for example, they are manufactured in two parts, top surface and bottom surface and subsequently joined. In this last step might appear a sliding between the top surface and the bottom surface having a small step on the leading edge or a small thickness gain can occur on the trailing edge. Normally these imperfections are corrected through a refill and/or sanding processes using many hours of manual labor.

Therefore the initial objective of this research is to determine the level of influence in the aerodynamic characteristics at low Reynolds numbers (Lissaman, 1981, Carmichael, 1981, Nagamatsu and Cuche, 1981, Schmitz, 1957, Cebeci, 1989, Mueller and Batill, 1982) of these imperfections in the manufacture, and determine whether there may be a value for which it would not be necessary to correct them.

2 EXPERIMENTAL SETUP

The experiments were performed in an open-circuit low-speed blow up wind tunnel located in aerodynamics laboratory managed by the Aerotecnia Department of Universidad Politecnica de Madrid. The wind tunnel has a test section with a 1.2 by 0.16 m cross section and several windows, including an optically transparent one. The wind tunnel has a contraction section upstream of the test section, with screen structures to provide uniform low-turbulent incoming flow to enter into the test section. Variation in the velocity distribution is less than 1% outside walls boundary layer and the mean turbulence level is less than 0.5%. The air speed in the test camera can be steadily regulated for values from 5 to 30 m/s and therefore test the airfoils up to 500,000 Reynolds numbers.

The airfoil used in the present study is a NACA0012 airfoil (Abbott and von Doenhoff, 1959). Two models have been built for tests, one of them used for forces measurement with an electronic force-balance of Plint Company measuring at 1,000 Hz during 4 seconds, and the other model is also provided with 33 pressure taps at its median span, connected to pressure scanner from Scanivalve Corporation. Pressure outputs were sampled at 500 Hz during 5 seconds for each measurement. Both models have been manufactured in a numerical control milling machine using chemical wood, with great stability and a good surface finish.

The models were manufactured in two separated parts, upper and lower part. For the study of the imperfections on the leading edge the models have a mechanism that allows scrolling the upper on the lower surface according to graduations in % of chord, as shown in Figure 1. The models have been tested from -4º to 26° angles of attack, and Reynolds

numbers (Re) of 75,000; 150,000; 300,000 and 450,000. For each case airfoils were studied with displacement of the upper on the lower surface of ±0.25%, ±0.5%, ±0.75% ±1.0% and ±1.5 %. The sign criteria used for displacement is positive when the upper surface moves backward (positive sense of the x-axis) and negative when it moves forward.

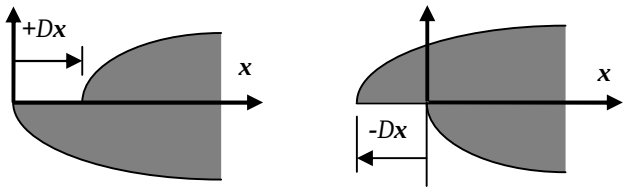

Figure 1. Leading edge step. Sign criteria used: positive when the upper surface moves backward and negative when moves forward.

For the study of the effect of trailing edge thickness (TE) both parts, upper and lower part, are able to be rotated around the leading edge using different gauges, in order to obtain the trailing edge thickness necessary, as shown in Figure 2. Models have been tested from 0º to 22° angles of attack, and at same Reynolds numbers. For each case airfoils were studied with trailing edge thickness to chord ratio of 2%, 4%, 6%, 8% and 10%.

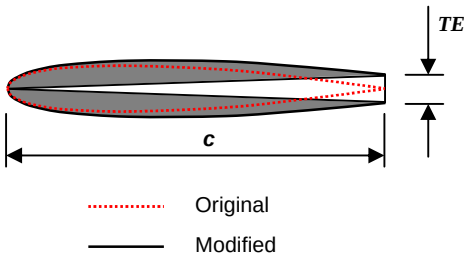

Figure 2. Trailing edge thickness.

The models have a 24 cm chord, allowing test up to the order of 450,000 Reynolds number with an air velocity of 30 m/s in the test section. Model span is 15.8 cm, whereas that of the wind tunnel test chamber wide is 16 cm. No special provision has been made to avoid the gap between model and wind tunnel walls, nor to correct measure results to take into account this effect (Allen and Vincenti, 1944) have been undertaken. It must be emphasized that the aim of this work is to compare the aerodynamic effect of different airfoil leading edge imperfections or trailing edge thicknesses.

In all cases the following measures were made: lift coefficient C_L, drag coefficient C_D, ¼ chord pitch moment $C_{M1/4}$, lift to drag ratio C_L/C_D , and upper and lower surface pressure distribution.

3 EXPERIMENTAL RESULTS

Experiments show (Ayuso et al, 2010) that at the same Reynolds number small values of leading edge displacement (Jones et al, 2008) cause an increase in the maximum C_L, for higher values the trend is to have lower maximum C_L values. If we study how the increase of the Reynolds number affects the maximum C_L we will see that it increases with the Reynolds number and this happens in different proportions for all studied steps. At the same Reynolds number the minimum C_D increases slightly as the size of the step increases. Looking at C_D variance with the Re shows that minimum C_D decreases for all steps in different magnitude. On lift to drag ratio shown for a same step, this increases with the Reynolds number, especially for small steps. At the same Re, C_L/C_D ratio decreases very slightly for small steps and more as the step size increases.

Figure 3 shows the effect of the step size on the lift coefficient along the angle of attack range at different Reynolds numbers and its influence in maximum C_L values.

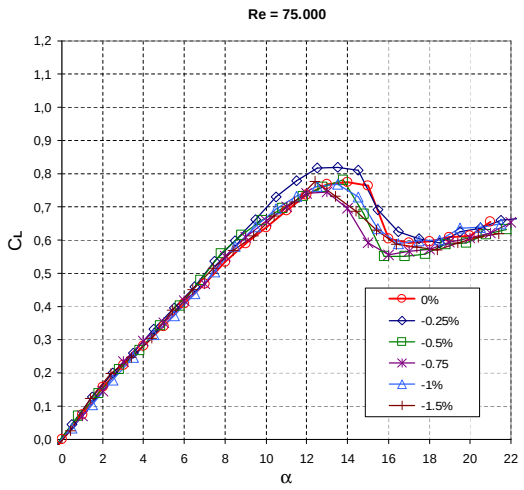

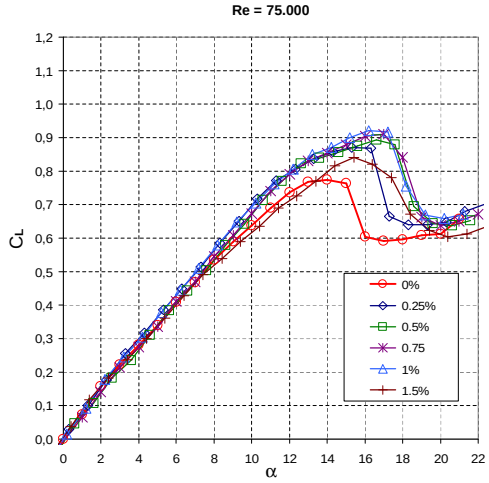

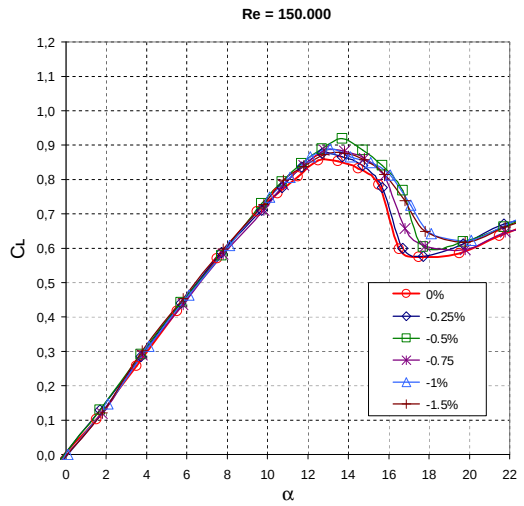

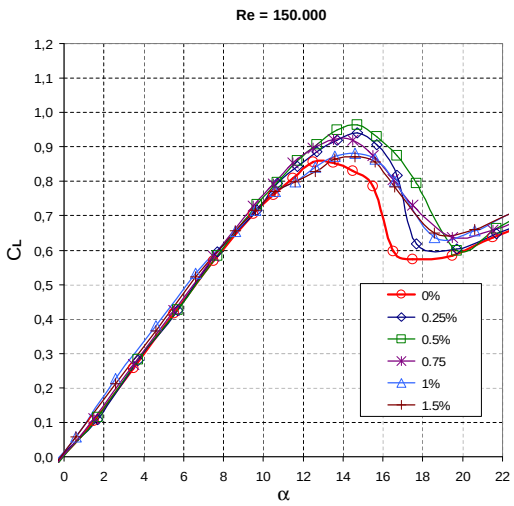

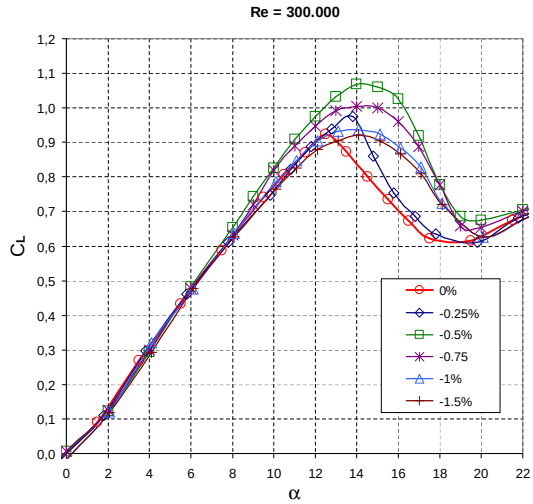

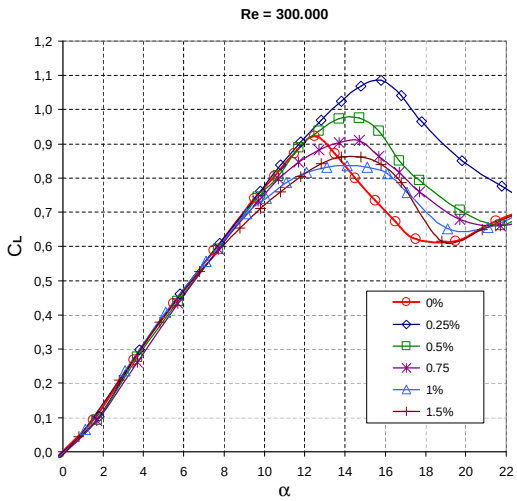

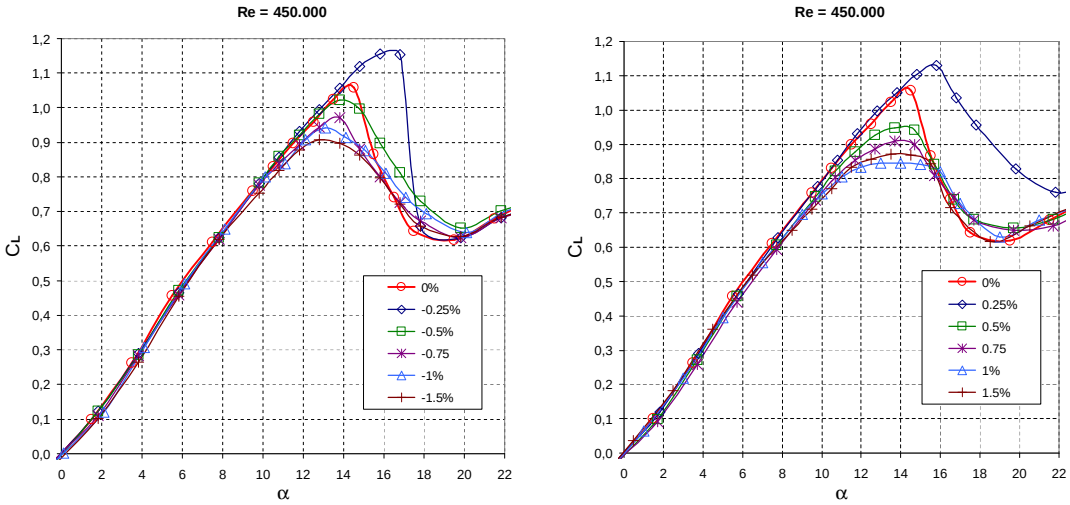

Figure 3. Effect of leading edge step, C_L versus angle of attack for negative and positive displacement Δx.

Figure 4 shows the effect of the step size on the drag coefficient at a fixed Reynolds number of 300,000 for positive displacement and the effect on the lift to drag ratio along the angle of attack range and its influence in maximum C_L/C_D values.

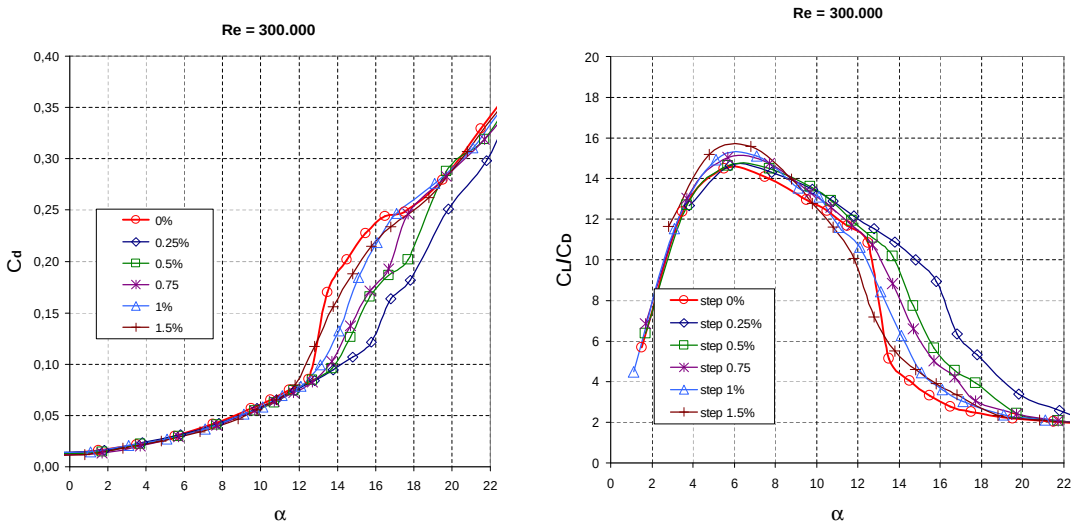

Figure 4. Effect of leading edge step. C_L versus angle of attack and C_L/C_D ratio versus angle of attack.

Pressure distributions along the airfoil chord for the nominal airfoil case and Re=3x10^5 is show in Fig. 5 (these distributions correspond to angles of attack close to the stalling angle). According to this plot, a laminar recirculation bubble appears at a = 10º, 12º and 13º (the short bubble is formed when de angle of attack is below 10 deg, see a high suction pressure near the leading edge followed by a plateau area and a sudden pressure recovery). The bubble is shorter and closer to the leading edge as the angle of attack increases (the leading edge suction peak increasing accordingly). At a = 14º the bubble shear layer can not reattach and the airfoil stalls (note that at a = 16º the boundary layer is separated in the whole airfoil upper surface). Same behavior is observed for displacement Δx of ±0.25% and ±0.50. For increasing values of the displacement the main difference is that the boundary layer separation starts at the trailing edge, as shown in figure 5.

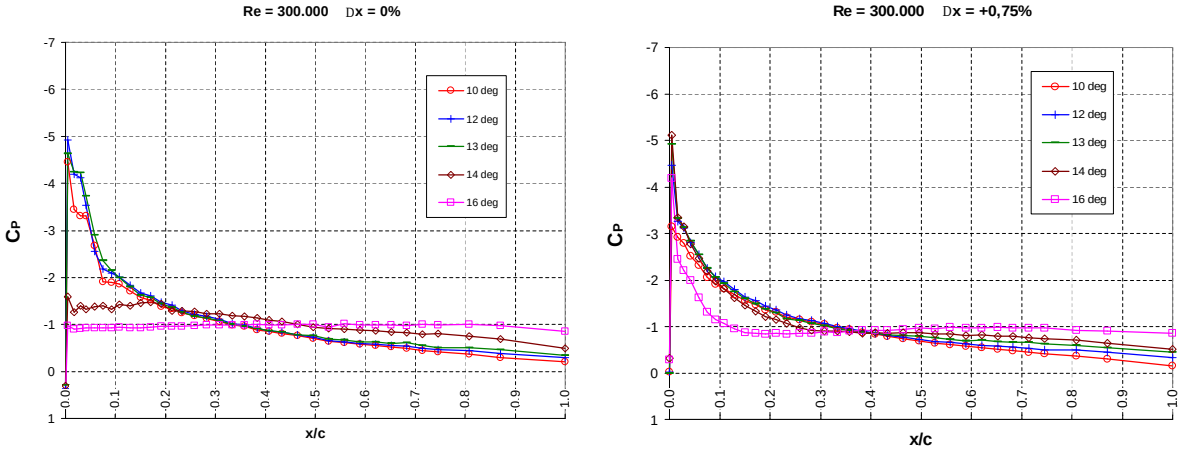

Figure 5. *Cp* distribution along the upper side. Re=300,000 and angles of attack close to the stalling angle of the nominal airfoil, Δx=0, and deformed airfoil, Δx= 0.75%.

On the other hand, when the trailing edge is open, the effect on C_L is shown in figure 6.

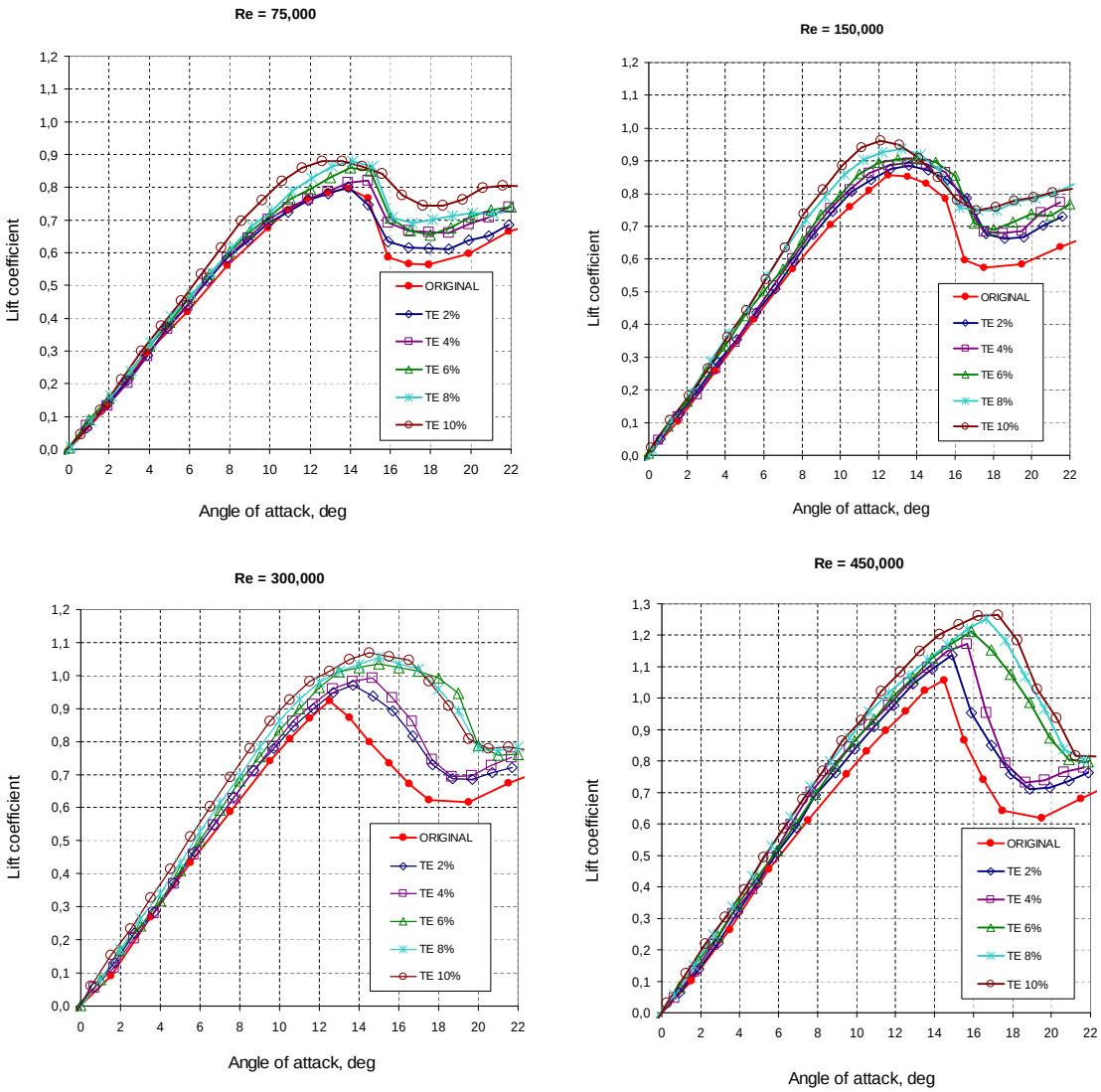

Figure 6. Effect of trailing edge size. C_L versus angle of attack for different trailing edge thickness (%).

Experiments show that at same Reynolds number small values of trailing edge thickness causes an increase in the maximum C_L (Sato and Yasuto, 1995, Standish and van Dam, 2003a, 2003b, Ramjee et al, 1986, Baker et al, 2008), for higher values of trailing edge thickness the trend is to have a limit in this maximum C_L values (Ramjee et al, 1986, Sato and Yasuto, 1995).

At a fixed Reynolds number the minimum C_D increases as the size of the trailing edge thickness increases (Sato and Yasuto, 1995, Ramjee et al, 1986, Baker et al, 2008). This increase in drag coefficient is bigger as the Reynolds number increases (Sato and Yasuto, 1995, Baker et al, 2008). Looking at the variation of C_D with Re shows that C_D decreases for all thicknesses as increase the Reynolds number (Ramjee et al, 1986).

Figure 7 shows the effect of the trailing edge thickness size on the drag coefficient as well as on lift to drag ratio at a fixed Reynolds number of 300,000 and their influence in maximum C_L/C_D value.

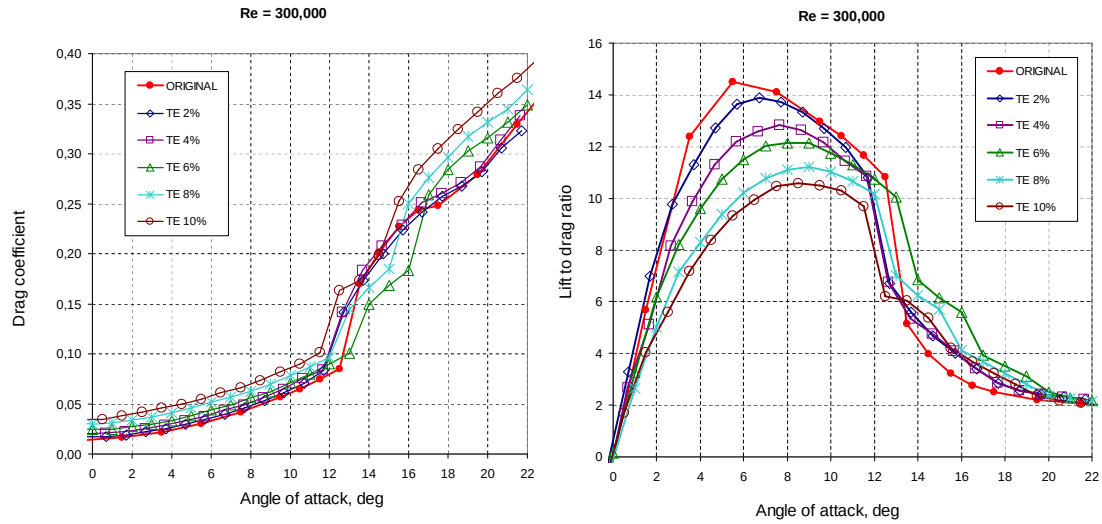

Figure 7. Effect of the trailing edge thickness. C_D and C_L/C_D ratio versus angle of attack.

For the lowest Reynolds number studied, Re=75x10^3, pressure distributions along the airfoil chord for the nominal airfoil case and several trailing edge studied are shown in Figure 8 (these distributions correspond to angles of attack close to the stalling angle). These plots suggest that the laminar burble after the suction peak is growing as the angle of attack increases, independently of the trailing edge thickness, so the stall is smooth.

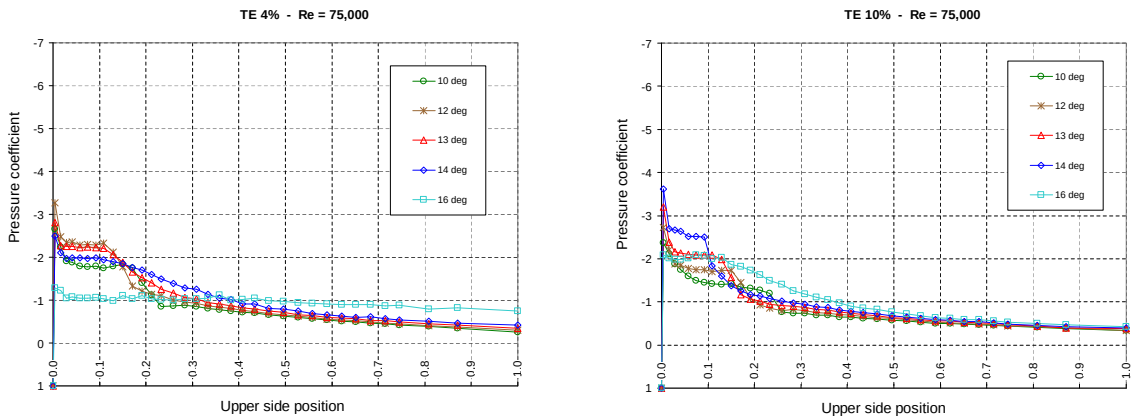

Figure 8. *Cp* distribution along the upper side, Re=75,000 and angles of attack close to the stalling angle.

For the highest Reynolds number studied, Re=450x10^3, pressure distributions along the airfoil chord corresponding to angles of attack close to the stalling angle are shown in Figure 9. These plots suggest that the behavior is similar to Reynolds number 300x10^3, so sudden stall occurs for original airfoil and small trailing edge thickness while smooth stall appears when the trailing edge thickness increases.

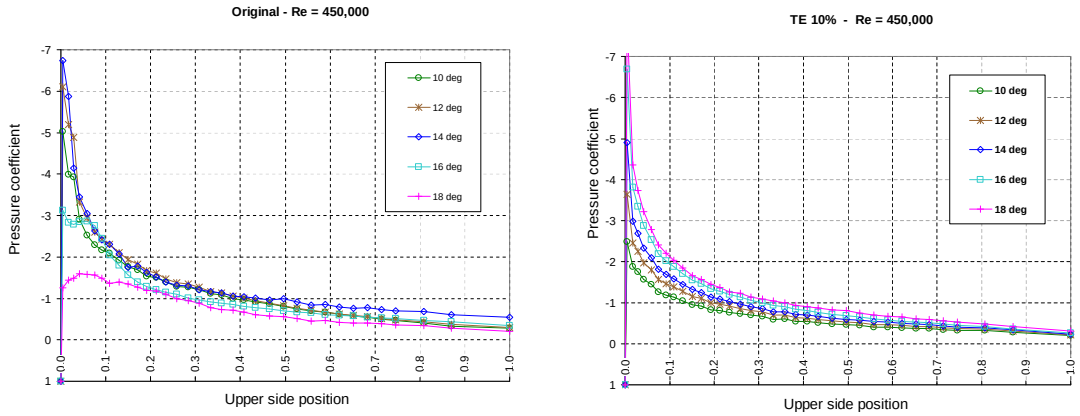

Figure 9. *Cp* distribution along the upper side, Re=450,000 and angles of attack close to the stalling angle.

4 CONCLUSIONS

The results show a degradation of the aerodynamic characteristics as the leading edge step size increases, bigger for the lowest values of studied Reynolds numbers and for positive displacement. However, only for certain combinations of step size and Re, aerodynamic performance seem to improve slightly. This is summarized in figure 10, and suggests that they could limit values of step that could be tolerated during manufacturing process, without that affecting considerably their aerodynamic features.

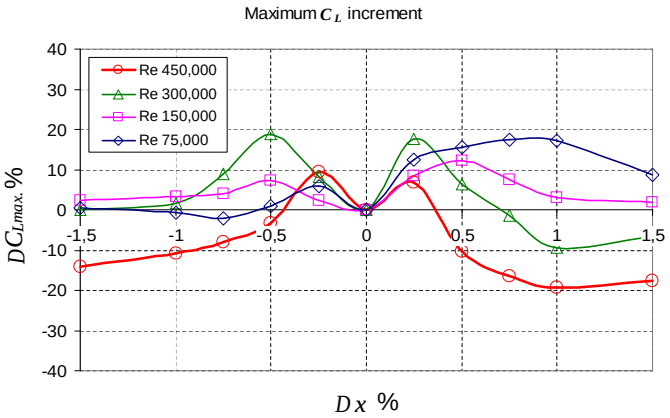

Figure 10. Increment in maximum lift coefficient (%) versus displacement Δx (%) at different Reynolds.

On the other hand, when the trailing edge of the profile is open, the results show a general improvement of aerodynamic lift as the trailing edge thickness size increases, as well as a bigger increase of drag so lift to drag ratio decreases (Fig 11). However, the general trend suggests that they could be limit value of tailing edge thickness that could be accepted during manufacturing process, without that affecting considerably their aerodynamic features.

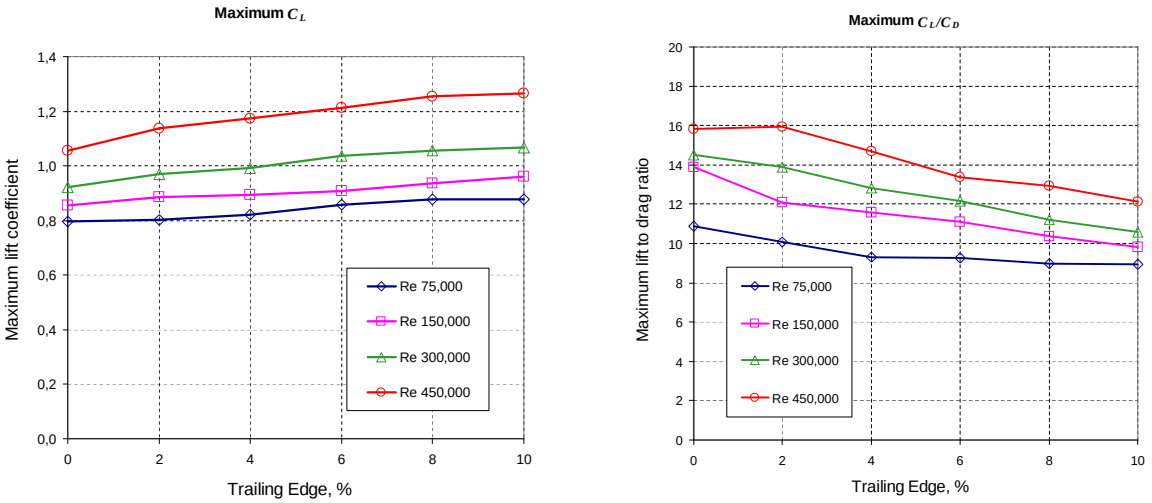

Figure 11. Increment in maximum C_L and maximum lift to drag ratio versus trailing edge thickness (%) at different Reynolds.

5 REFERENCES

Journal papers:

Ayuso, L., Sant, R. and Meseguer, J., 2010. Aerodynamic study of airfoils with leading edge imperfections at low Reynolds number. 40th Fluid Dynamics Conference and Exhibit, Chicago, Illinois, AIAA 2010-4625.

Baker, Jonathon P., van Dam, C.P., and Gilbert, Benson L., 2008. Flatback airfoil wind tunnel experiment, Sandia Report SAND2008.

Carmichael, B.H., 1981. Low Reynolds number airfoil survey. NASA CR-165803, Vol.1.

Cebeci, T., 1989. Essential ingredients of a method for low Reynolds number airfoils, AIAA Journal, Vol.27, No.12, 1680-1688.

Jones, A.R., Bahktian, N.M. and Babinsky, H., 2008. Low Reynolds number aerodynamics of leading-edge flaps, Journal of Aircraft, Vol.45, No.1, 342-345.

Junzo Sato and Yasuto Sunada, 1995. Experimental research on blunt trailing-edge airfoil sections at low Reynolds number, AIAA Journal, Vol.33, No.11, 2001-2005.

Lissaman, P.B.S., 1983. Low Reynolds number airfoils. Annual Review of Fluid Mechanics, Vol.15, 223-239.

Mueller, T.J. and Batill, S.M., 1982. Experimental studies of separation on a two-dimensional airfoil at low Reynolds number, AIAA Journal, Vol.20, No.4. 457-463.

Nagamatsu, H.T., and Cuche, D.E., 1981. Low Reynolds number aerodynamics characteristics of low-drag NACA 63-208 airfoil, Journal of Aircraft, Vol.18, No.10, 833-837.

Ramjee, V., Tulapurkara, E.G. and Balabaskaran, V., 1986. Experimental and theoretical study of wings with blunt trailing edge. AIAA Journal of Aircraft Vol. 23, No.4. Engineering Notes, 349-352.

Schmitz, F.W., 1957. Aerodynamik des flugmodells, Verlag, Duisburg, Germany.

Standish, K.J. and van Dam, C.P., 2003a. Analysis of blunt trailing edge airfoils. AIAA 41st Aerospace Sciences Meeting and Exhibit.

Standish, K.J. and van Dam, C.P., 2003b. Aerodynamic analysis of blunt trailing edge airfoils, Journal of Solar Energy Engineering, Vol 125, Issue 4, 479-488,

Monographs, Multi-author volumes, Proceedings:

Abbott, I.H., and von Doenhoff, A.E., Theory of wing sections, Dover, New York, 1959.

Allen, H. J., and Vincenti, W. G., Wall Interference in a Two-Dimensional-Flow Wind Tunnel, with Consideration of compressibility, NACA Rept. 782, 1944.

Berg, Dale E. and Barone, Matthew, 2008, Aerodynamic and aeroacoustic properties of a flatback airfoil, WINDPOWER, June, Houston, USA.